

Intelligent Deep Transfer Learning Based Malaria Parasite Detection and Classification Model Using Biomedical Image

Ahmad Alassaf and Mohamed Yacin Sikkandar*

Department of Medical Equipment Technology, College of Applied Medical Sciences, Majmaah University, Al Majmaah, 11952, Saudi Arabia

*Corresponding Author: Mohamed Yacin Sikkandar. Email: m.sikkandar@mu.edu.sa

Received: 29 November 2021; Accepted: 09 February 2022

Abstract: Malaria is a severe disease caused by Plasmodium parasites, which can be detected through blood smear images. The early identification of the disease can effectively reduce the severity rate. Deep learning (DL) models can be widely employed to analyze biomedical images, thereby minimizing the misclassification rate. With this objective, this study developed an intelligent deep-transfer-learning-based malaria parasite detection and classification (IDTL-MPDC) model on blood smear images. The proposed IDTL-MPDC technique aims to effectively determine the presence of malarial parasites in blood smear images. In addition, the IDTL-MPDC technique derives median filtering (MF) as a pre-processing step. In addition, a residual neural network (Res2Net) model was employed for the extraction of feature vectors, and its hyperparameters were optimally adjusted using the differential evolution (DE) algorithm. The k -nearest neighbor (KNN) classifier was used to assign appropriate classes to the blood smear images. The optimal selection of Res2Net hyperparameters by the DE model helps achieve enhanced classification outcomes. A wide range of simulation analyses of the IDTL-MPDC technique are carried out using a benchmark dataset, and its performance seems to be highly accurate (95.86%), highly sensitive (95.82%), highly specific (95.98%), with a high F1 score (95.69%), and high precision (95.86%), and it has been proven to be better than the other existing methods.

Keywords: Computer-aided diagnosis; malaria parasites; biomedical images; blood smear images; deep learning

1 Introduction

Malaria is a life-threatening disease caused by the Plasmodium parasite, and is a serious health concern worldwide. According to reports by the World Health Organization (WHO) in 2017, nearly 219 million cases of malaria occurred in 87 countries worldwide [1]. The WHO selected the Eastern Mediterranean, Western Pacific, Americas, and Southeast Asia as high-risk regions. Malaria is curable and can be prevented when appropriate measures and initiatives are effectively taken, which rely mainly on earlier diagnoses of the malaria parasite [2]. Various methods have been reported to detect malarial



This work is licensed under a Creative Commons Attribution 4.0 International License, which permits unrestricted use, distribution, and reproduction in any medium, provided the original work is properly cited.

parasites in the blood, such as microscopic diagnosis, medical diagnosis [3], polymerase chain reaction (PCR), and rapid diagnostic test (RDT) [4].

Traditional diagnostic approaches such as PCR and other clinical diagnostic methods are dependent on experimental settings; eventually, the accuracy and efficiency depend significantly on the purely subjective knowledge of individuals. This limited knowledge is unable to reach remote locations where malaria could be predominant. Microscopic diagnosis and the RDT are effective malaria diagnostic technologies that make a large contribution to malaria control in the present scenario [5]. The RDT is a powerful diagnostic method that does not require any microscope or trained professionals and can offer diagnoses within 15 min. However, the RDT method has some limitations, including the inability to quantify parasite density, low sensitivity, susceptibility to damage by heat and humidity, high cost compared with light microscopy, and inability to differentiate between *Plasmodium malariae*, *P. vivax*, and *P. ovale*. These drawbacks can be overcome by the microscopic system and thus it is categorized as an efficient method to detect malarial parasites but requires the presence of a professional microscopist [6].

Microscopic inspection is considered a primary and typical technique for malaria diagnosis [7] to detect the occurrence of parasites from a blood drop in a thick blood smear. The investigation accuracy is based on an efficient technician examining and classifying the parasitized and uninfected blood cells found in the blood smear. Automated microscopic malaria parasite diagnosis could be a powerful diagnostic method that includes segmentation of cells and classification of infected cells and the acquisition of microscopic blood smear images [8]. It should be noted that the effective identification of malarial parasites and segmentation of blood cells could be utilized to carry out counting.

Conventional methods for malaria diagnosis are time consuming, might create incorrect reports because of human errors, and are not suitable for wide-ranging diagnosis. This motivated us to present an automated diagnosis of malaria using deep-learning (DL) algorithms. Various concepts exist towards the recognition of malaria parasites in microscopic images via a pre-trained variant of a convolutional neural network (CNN) [9,10]. Chakradeo et al. [11] introduced a visual geometry group (VGG)-based approach and compared it with previously presented methods for identifying diseased cells. It exceeds the accuracy of most previously presented methods in a range of metrics. Hence, it reduces the computational time and consumption of technical resources.

Fuhad et al. [12] presented an automatic CNN-based algorithm for malaria detection using microscopic blood smears. This involves different methods, such as data augmentation, knowledge distillation, and feature extraction. An autoencoder is categorized as a support vector machine (SVM) or k -nearest neighbor (KNN). CNN models execute the training process at three levels, autoencoder training, general training, and distillation training, to improve and optimize the inference performance and model accuracy.

Researchers have designed a traditional CNN method to distinguish between infected and healthy blood samples [13]. The proposed method contains fully connected (FC) layers and three convolutional layers. The neural network system proposed a cascade of numerous convolution layers having different filters existing in each layer that produces better accuracy according to the available resources. The method was implemented on various blood sample images to investigate its accuracy.

Li et al. [14] presented a DL method to detect malaria parasites at different levels from blood smears with deep transfer to a graph convolution network (DTGCN). This is the primary application of the graph convolution network (GCN) model for multistage malaria parasite detection in an image. Rahman et al. [15] converted a malaria parasite object recognition dataset to data classification, which makes it the prime malaria classification dataset, and estimated the performance of many advanced

deep neural network (DNN) frameworks pre-trained on medical and normal images on this novel dataset. Researchers analyzed the effects of pre-processing and found that a custom architecture, VGG-16, and a residual neural network (ResNet) formed in an earlier study have been employed [16]. The pre-processing method was investigated, which includes comprehensive normalization and gray-world normalization.

In this study, we developed an intelligent deep transfer learning-based malaria parasite detection and classification (IDTL-MPDC) model using blood-smear images. In addition, the IDTL-MPDC technique derives median filtering (MF) as a pre-processing step. The Res2Net model was employed for the extraction of feature vectors, and its hyperparameters were optimally adjusted using the differential evolution (DE) algorithm. Furthermore, the KNN classifier was used to assign appropriate classes to the blood smear images. The optimal selection of Res2Net hyperparameters by the DE model helps achieve enhanced classification outcomes. A wide range of simulation analyses of the IDTL-MPDC technique were performed using a benchmark dataset.

2 The Proposed Model

In this study, a new IDTL-MPDC technique was developed to effectively determine the presence of malarial parasites using blood smear images. The IDTL-MPDC technique involves various sub-processes, namely, MF-based pre-processing, Res2Net-based feature extraction, DE-based hyperparameter optimization, and KNN-based classification.

2.1 Pre-processing Using the MF Technique

The major drawback of the blood smear image is the poor quality of the image owing to spot noise. Spot noise is a disadvantage because it affects single interpretation and recognition processes and undermines the image quality. Consequently, point refining is a major phase in the recognition, extraction, and analysis of healthcare images. In various effective approaches for removing noise from healthcare images, the MF technique is used because of its specificity, which has applications in healthcare image noise elimination [17]. The basic concept behind the median filter is to introduce an $m \times n$ neighborhood to select the median value of the ordered number, replace the central pixel, and assemble each neighborhood in ascending order. This can be expressed as

$$y_{(m,n)} = \text{median}\{x_{(i,j)}, (i, j) \in C\}, \quad (1)$$

where C signifies the neighborhood centered around the position (m, n) of an image. In this study, median filtering was adopted to remove digital noise from the input image, and a filter mask with a size of 3×3 was applied.

2.2 Feature Extraction Using the Res2Net Model

Next, the pre-processed blood smear image is passed to the Res2Net model to derive the feature vectors. The Res2Net block [18] is different from ResNet, which utilizes many sets of convolution functions and concepts of hierarchical influences in a single remaining block. It is distinct from the multi-scale feature removal techniques that use a layer-wise approach, as the Res2Net block removes multi-scale features at the granular level and improves the range of receptive domains of every convolution layer.

As illustrated in Fig. 1, an input is primarily referred to as a group of 1×1 convolution kernels, and the resultant feature maps are separated into four sets, followed by 1×1 convolution. The primary set of feature maps x_1 has no convolutional function. In the secondary set of feature maps x_2 , a group

of 3×3 convolution kernels is utilized for extracting the feature in it, and the outcome is y_2 . Then, y_2 and the tertiary set of feature maps x_3 are aimed at the secondary group of 3×3 convolution kernels, and the outcome is y_3 . Subsequently, y_3 and the quarter set of feature maps x_4 are aimed at the tertiary set of 3×3 convolution kernels, and the outcome is y_4 . Eventually, the resultant feature map in every set is concatenated and aimed at other groups of 11 convolution kernels to fuse the feature. Related to the residual block under ResNet, Res2Net utilizes the remaining link to connect the input to the outcome of the final set of convolutional functions. As the input feature is changed to the resultant features with several paths, the receptive domains are improved if the group of convolution kernels is passed.

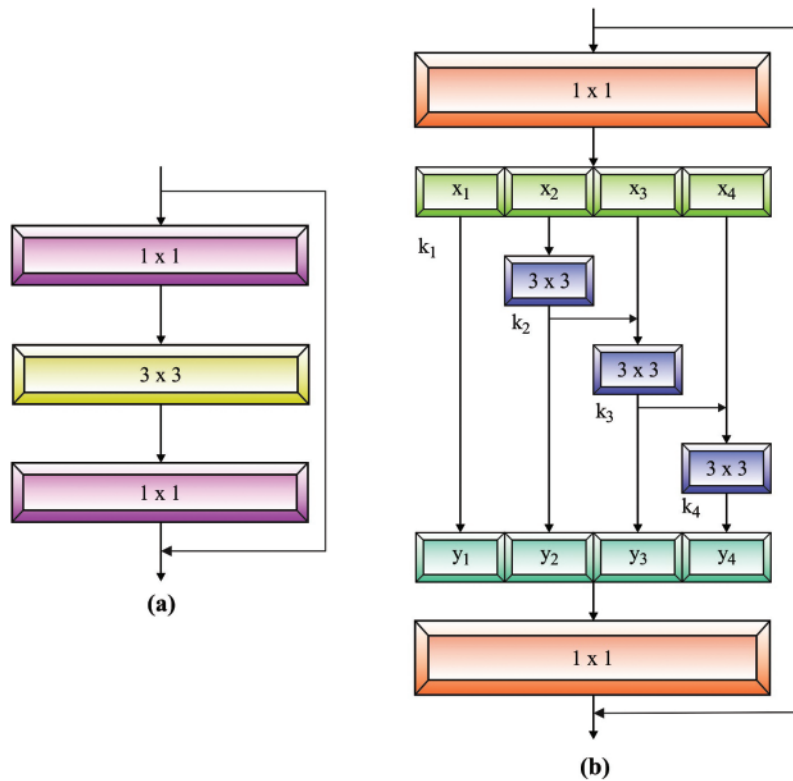


Figure 1: (a) ResNet Model (b) Res2Net Model

2.3 Hyperparameter Tuning Using the DE Technique

The DE technique can be utilized to optimally adjust the hyperparameters of the Res2Net model. The DE technique has primarily been established in [19]. The vital model after the DE technique is a process to create a testing parameter vector and more weight variance between two population vectors to the third one. As another evolutionary technique, the DE approach aims at developing a population of N_p , D dimension parameter vectors that are assumed as individuals that encode the candidate solution, for instance,

$$\vec{x}_{i,g} = \{x_{1,i,g}, x_{2,i,g}, \dots, x_{D,i,g}\}, \quad (2)$$

where $i = 1, 2, 3 \dots, N_p$.

Step 1: Initialize every individual arbitrarily (in bounds -2 and $+2$) of N_p population

$$\vec{x}_{i,g} = \{x_{1,i,g}, x_{2,i,g}, \dots, x_{D,i,g}\}; \text{ where } i = 1, 2, 3, \dots, N_p. \quad (3)$$

Step 2: Mutation:

For $i = 1$ to N_p , we create the mutation vector $\vec{v}_{i,g} = \{v_{1,i,g}, v_{2,i,g}, \dots, v_{D,i,g}\}$ equivalent to the target vector $\vec{x}_{i,g}$ using

$$\text{“DE/rand - to - best/1 : } \vec{v}_{i,g} = \vec{x}_{i,g} + F(\vec{x}_{\text{best},g} - \vec{x}_{i,g}) + F(\vec{x}_{r'_1,g} - \vec{x}_{r'_2,g}) \quad (4)$$

The optimum value of F defined in this study was equivalent to 0.5.

Step 3: Crossover:

Generate testing vector $\vec{u}_{i,g}$ to all target vectors $\vec{x}_{i,g}$, where

$\vec{u}_{i,g} = \{u_{1,i,g}, u_{2,i,g}, \dots, u_{D,i,g}\}$ as follows:

for $i = 1$ to N_p , $j_{Rand} = [rand(0, 1) * D]$; for $j = 1$ to D .

$$u_{i,j,g} = \begin{cases} v_{j,i,g} & \text{if } (rand_{ij}(0, 1) \leq C_r) \\ x_{i,j,g} & \text{otherwise.} \end{cases} \quad (5)$$

end

Step 4: Selection:

for $i = 1$ to N_p ,

$$\vec{x}_{i,g+1} = \begin{cases} \vec{u}_{i,g} & \text{if } f(\vec{u}_{i,g}) \leq f(\vec{x}_{i,g}) \\ \vec{x}_{i,g} & \text{otherwise.} \end{cases} \quad (6)$$

end

Step 5: Increase the generation number $g = g + 1$.

Because the generation cycle is repeated in Step 2, the maximum number of generation cycles is attained. The great minimal error fitness and its equivalent better vectors containing $(N/2 + 1)$ amount of $h(n)$ coefficient are defined. Eventually, an entire optimum filter coefficient equivalent to $(N + 1)$ is attained by copy and concatenation of beyond coefficients to obtain the last optimum frequency spectrum of the finite impulse response (FIR) filter.

Algorithm 1: Pseudocode of DE

Create primary population $P^0 = \{\vec{x}_1^0, \vec{x}_2^0, \dots, \vec{x}_N^0\}$

Assume $t = 0$

repeat

for all individuals \vec{x}_i^t from the population P^t do

Create 3 arbitrary integers r_1, r_2 and $r_3 \in \{1, 2, \dots, N\} \setminus i$, with $r_1 \neq r_2 \neq r_3$

Create an arbitrary integer $j_{rand} \in \{1, 2, \dots, D\}$

for all parameters j do

(Continued)

Algorithm 1: Continued

$$u_{ij}^{t+1} = \begin{cases} x_{r_{3,j}}^t + F \times (x_{r_{1,j}}^t - x_{r_{2,j}}^t), & \text{if } (rand \leq CR | j = rand[1, D]) \\ x_{ij}^t, & \text{otherwise} \end{cases}$$

end for
Change \bar{x}_i^t with child \bar{u}_i^{t+1} from the population P^{t+1} ,
if \bar{u}_i^{t+1} is optimum, otherwise \bar{x}_i^t has maintained
end for
 $t = t + 1$
until the end criteria were attained

2.4 Image Classification Using the KNN Technique

In the last stage, the KNN model receives the features as input and projects proper class labels. KNN is a simple machine learning (ML) technique. To define the classification of the testing data, KNN executes a test to check the amount of similarity among k trained data and documents to save a specific number of classified information [20]. As KNN categorizes instances, in this work, it would be benign and malicious code instances near the training space. The classification of unknown instances can be implemented by evaluating the distance between the unknown instances and training instances. As the instance is categorized according to the majority vote of neighbor, the most widespread neighbor is evaluated by a distance function. When $k=1$, the instance is allocated to the class of its adjacent neighbors. In n -dimensional space, distance between x and y can be attained by a distance function defined as follows:

$$\sqrt{\sum_{i=1}^k (x_i - y_i)^2}. \quad (7)$$

3 Experimental Validation

To examine the malaria detection performance of the IDTL-MPDC technique, an experimental result analysis was performed on the open-access malaria dataset. It comprises 27558 cell images under two categories, parasitized and uninfected cells, with identical numbers of samples, as shown in Fig. 2.

Tab. 1 lists the overall malaria classification results of the IDTL-MPDC technique under varying epoch counts.

Fig. 3 presents a brief $accu_y$ analysis of the IDTL-MPDC technique in the presence of distinct epochs. The figure shows that the IDTL-MPDC technique achieves better $accu_y$ values for every epoch. For instance, the IDTL-MPDC technique achieved $accu_y$ of 95.85% and 95.41% under lower epoch counts of 100 and 200, respectively. Similarly, the IDTL-MPDC technique achieved $accu_y$ of 95.59% and 95.46% under maximum epoch counts of 900 and 1000, respectively.

A detailed $sens_y$ and $spec_y$ analysis of the IDTL-MPDC technique with various epochs is shown in Fig. 4. The results revealed that the IDTL-MPDC technique offered increased values of $sens_y$ and $spec_y$. For instance, with 100 epochs, the IDTL-MPDC technique has obtained $sens_y$ and $spec_y$ of 95.67% and 95.99%, respectively. Simultaneously, with 400 epochs, the IDTL-MPDC manner has achieved $sens_y$ and $spec_y$ of 95.86% and 95.81%, respectively. Moreover, after 700 epochs, the IDTL-MPDC technique achieved $sens_y$ and $spec_y$ of 95.19% and 95.46%, respectively. Eventually, after 1000 epochs, the IDTL-MPDC algorithm achieved $sens_y$ and $spec_y$ of 95.46% and 95.09%, respectively.

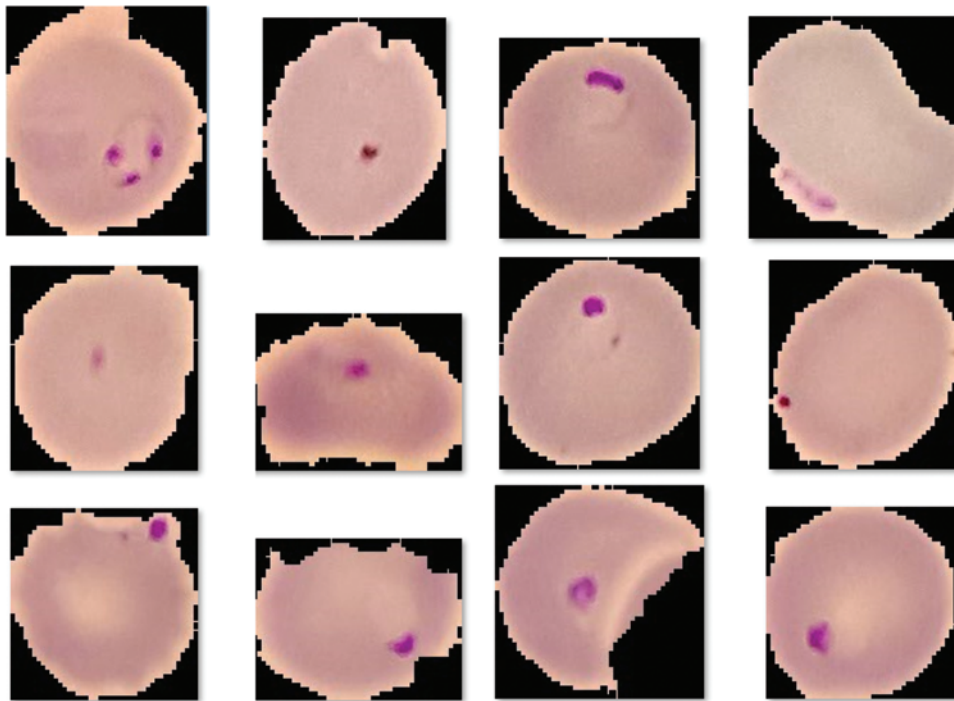


Figure 2: Sample images

Table 1: Malaria classification results analysis of IDTL-MPDC technique

No. of Epochs	Precision	Sensitivity	Specificity	Accuracy	F1 score
100	95.85	95.67	95.99	95.85	95.00
200	95.01	95.45	95.14	95.41	95.93
300	95.53	95.47	95.17	95.51	95.17
400	95.48	95.86	95.81	95.67	95.52
500	95.08	95.77	95.70	95.73	95.29
600	95.86	95.82	95.98	95.86	95.69
700	95.04	95.19	95.46	95.06	95.13
800	95.50	95.17	95.68	95.42	95.71
900	95.65	95.57	95.35	95.59	95.40
1000	95.47	95.46	95.09	95.46	95.05

A comprehensive $prec_n$ and $F1_{score}$ analysis of the IDTL-MPDC system with varying epochs is shown in Fig. 5. The results show that the IDTL-MPDC methodology can improve the values of $prec_n$ and $F1_{score}$. For example, with 100 epochs, the IDTL-MPDC methodology obtained $prec_n$ and $F1_{score}$ of 95.85% and 95%, respectively. Simultaneously, with 400 epochs, the IDTL-MPDC technique achieved $prec_n$ and $F1_{score}$ of 95.48% and 95.52%, respectively. Moreover, after 700 epochs, the IDTL-MPDC system achieved $prec_n$ and $F1_{score}$ of 95.04% and 95.13%, respectively. Eventually, after 1000 epochs, the IDTL-MPDC technique obtained $prec_n$ and $F1_{score}$ of 95.47% and 95.05%, respectively.

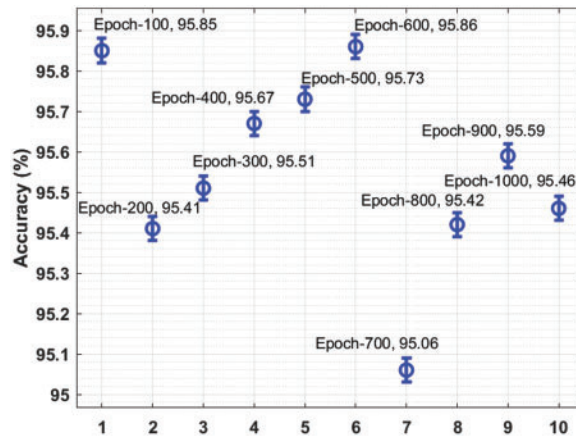


Figure 3: Result analysis of the IDTL-MPDC technique in terms of accuracy

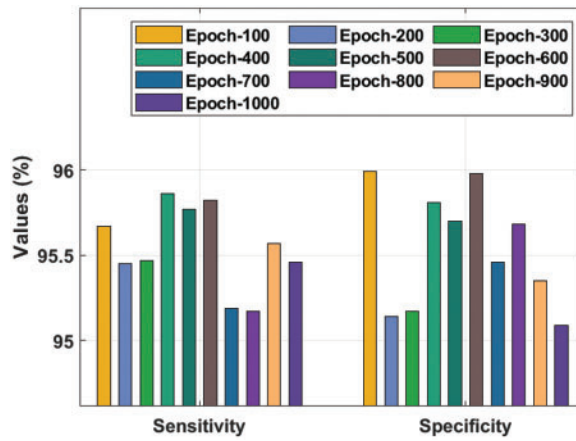


Figure 4: Result analysis of the IDTL-MPDC technique in terms of sen_y and $spec_y$

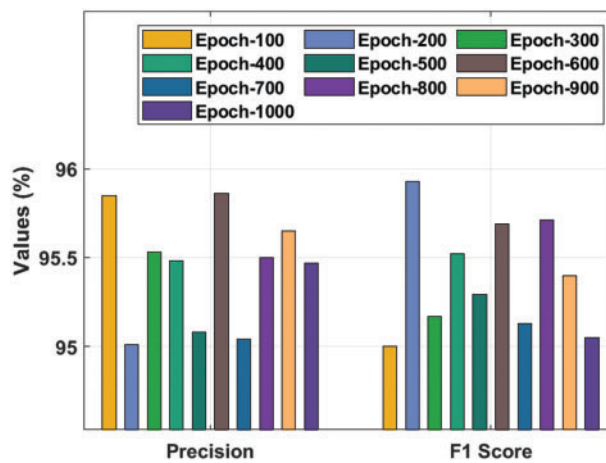


Figure 5: Result analysis of the IDTL-MPDC technique in terms of $prec_n$ and $F1_{score}$

Fig. 6 depicts the receiver operating characteristic (ROC) curve analysis of the use of the IDTL-MPDC technique on the test dataset. The figure states that the IDTL-MPDC technique has attained improved outcomes with the maximal ROC of 98.6290.

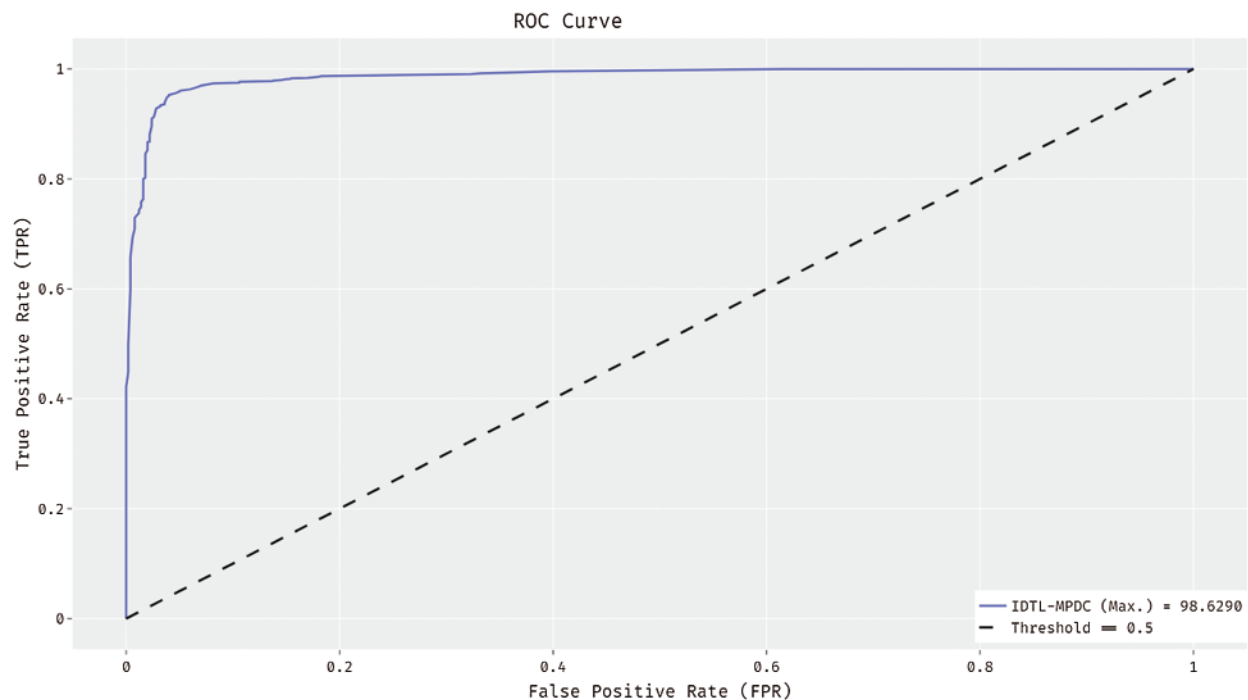


Figure 6: ROC analysis of IDTL-MPDC technique

Fig. 7 shows the ROC analysis of the IDTL-MPDC technique on the test dataset. The figure exposed that the IDTL-MPDC technique has reached an enhanced outcome with the minimum ROC of 97.9295.

Tab. 2 provides an extensive comparative analysis of the IDTL-MPDC technique with other recent methods [21]. Fig. 8 depicts the $accu_y$ analysis of the IDTL-MPDC technique with other techniques. The figure shows that the AIPM-CM and ML-ASM techniques have lower $accu_y$ values of 73% and 84%, respectively. This is followed by the Inception-v3, You only look once (YOLO)v3, YOLO-v4, and Faster Region-Based Convolutional Neural Network (RCNN) models that exhibit moderate $accu_y$ values of 93.06%, 93.15%, 94.75%, and 93.26%, respectively. However, the IDTL-MPDC technique has outperformed the other techniques with a maximum $accu_y$ of 95.86%.

Fig. 9 illustrates the $F1_{score}$ analysis of the IDTL-MPDC method with other algorithms. The figure clearly shows that the AIPM-CM and ML-ASM techniques have reduced $F1_{score}$ values of 79% and 81%, respectively. In addition, the Inception-v3, YOLO-v3, YOLO-v4, and Faster R-CNN models displayed moderate $F1_{score}$ values of 93.06%, 92%, 91%, and 89.71%, respectively. The IDTL-MPDC model outperformed the other approaches with a maximum $F1_{score}$ of 95.69%.

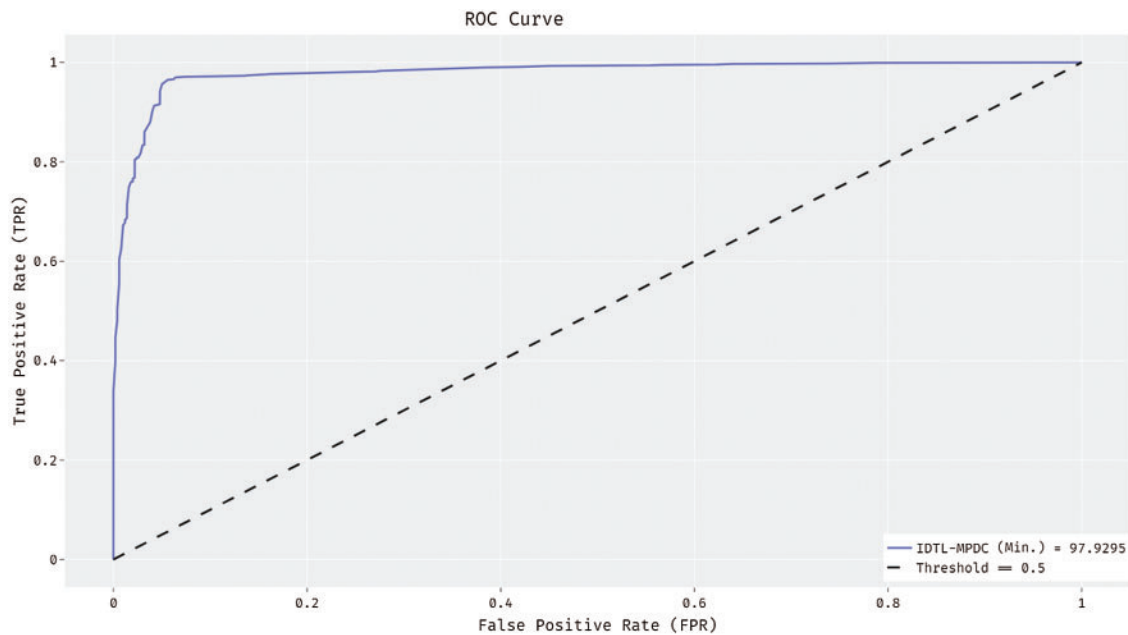


Figure 7: ROC analysis of IDTL-MPDC technique

Table 2: Comparative analysis of the IDTL-MPDC technique with different measures

Method	Accuracy	Sensitivity	Specificity	F1 score	Precision
AIPM-CM	73.00	85.00	72.00	79.00	76.00
ML-ASM	84.00	98.10	68.90	81.00	83.00
Inception-v3 model	93.06	92.97	93.13	93.06	93.06
YOLO-V3	93.15	92.00	93.25	92.00	91.00
YOLO-V4	94.75	92.00	95.23	92.00	92.00
Faster R-CNN	93.26	86.90	94.25	89.71	92.70
IDTL-MPDC	95.86	95.82	95.98	95.69	95.86

Fig. 10 depicts the $prec_n$ analysis of the IDTL-MPDC technique with other techniques. The figure stated that the AIPM-CM and ML-ASM techniques have portrayed lower $prec_n$ values of 76% and 83%, respectively. The Inception-v3, YOLO-v3, YOLO-v4, and Faster RCNN models have demonstrated moderate $prec_n$ values of 93.06%, 91%, 92%, and 92.7%, respectively. The IDTL-MPDC technique outperformed the other methods with a maximal $prec_n$ of 95.86%.

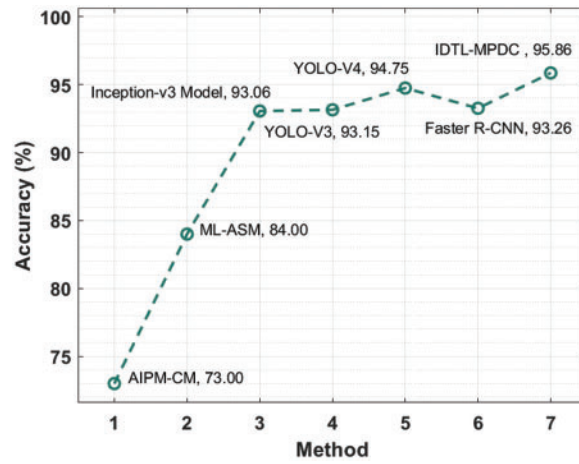


Figure 8: Acc_y analysis of the IDTL-MPDC technique with other existing approaches

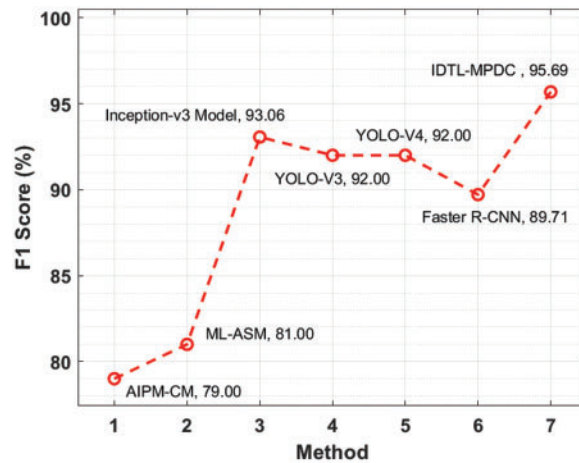


Figure 9: $F1_{score}$ analysis of the IDTL-MPDC technique with other existing approaches

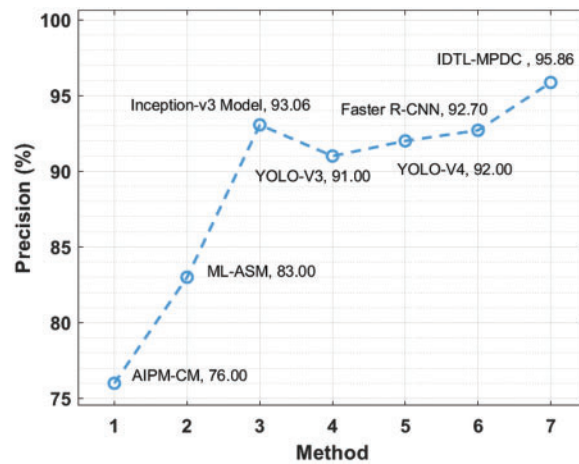


Figure 10: $Prec_n$ analysis of the IDTL-MPDC technique with other existing approaches

4 Conclusion

In this study, a new IDTL-MPDC technique has been proposed to effectively determine the presence of malarial parasites in blood smear images. The IDTL-MPDC technique involves various sub-processes, namely, MF-based pre-processing, Res2Net-based feature extraction, DE-based hyperparameter optimization, and KNN-based classification. The optimal selection of Res2Net hyperparameters by the DE model helps achieve enhanced classification outcomes. A wide range of simulation analyses of the IDTL-MPDC technique have been carried out using a benchmark dataset, and the simulation results reported better outcomes than other related techniques. Therefore, the IDTL-MPDC technique can be utilized as a proficient tool for the detection and classification of malarial parasites. In the future, deep instance segmentation techniques should be included to improve the classification performance of the IDTL-MPDC technique.

Acknowledgement: The authors extend their appreciation to the Deanship of Scientific Research at Majmaah University for funding this study under project number R-2022-76.

Funding Statement: The authors received no specific funding for this study.

Conflicts of Interest: The authors declare that they have no conflicts of interest regarding this study.

References

- [1] Fact Sheet about Malaria. 2019. Available online: <https://www.who.int/news-room/fact-sheets/detail/malaria>.
- [2] I. M. Masanja, M. L. McMorrow, M. B. Maganga, D. Sumari, V. Udhayakumar *et al.*, “Quality assurance of malaria rapid diagnostic tests used for routine patient care in rural Tanzania: Microscopy versus real-time polymerase chain reaction,” *Malaria Journal*, vol. 14, no. 1, pp. 85, 2015.
- [3] M. Poostchi, K. Silamut, R. J. Maude, S. Jaeger and G. Thoma, “Image analysis and machine learning for detecting malaria,” *Translational Research*, vol. 194, pp. 36–55, 2018.
- [4] E. I. Obeagu, C. Uo and E. Is, “Malaria rapid diagnostic test (RDTs),” *Annals of Clinical & Laboratory Science*, vol. 6, no. 4:275, pp. 1–3, 2018.
- [5] B. A. Mathison and B. S. Pritt, “Update on malaria diagnostics and test utilization,” *Journal of Clinical Microbiology*, vol. 55, no. 7, pp. 2009–2017, 2017.
- [6] S. Rajaraman, S. K. Antani, M. Poostchi, K. Silamut, M. A. Hossain *et al.*, “Pre-trained convolutional neural networks as feature extractors toward improved malaria parasite detection in thin blood smear images,” *PeerJ*, vol. 6, pp. e4568, 2018.
- [7] J. A. Quinn, R. Nakasi, P. K. Mugagga, P. Byanyima, W. Lubega *et al.*, “Deep convolutional neural networks for microscopy-based point of care diagnostics,” in *Proc. of the Machine Learning for Healthcare Conf.*, Los Angeles, CA, vol. 56, pp. 271–281, 2016.
- [8] D. Yang, G. Subramanian, J. Duan, S. Gao, L. Bai *et al.*, “A portable image-based cytometer for rapid malaria detection and quantification,” *PLoS ONE*, vol. 12, no. 6, pp. e0179161, 2017.
- [9] J. E. Arco, J. M. Górriz, J. Ramírez, I. Álvarez and C. G. Puntonet, “Digital image analysis for automatic enumeration of malaria parasites using morphological operations,” *Expert Systems with Applications*, vol. 42, no. 6, pp. 3041–3047, 2015.
- [10] D. Bibin, M. S. Nair and P. Punitha, “Malaria parasite detection from peripheral blood smear images using deep belief networks,” *IEEE Access*, vol. 5, pp. 9099–9108, 2017.
- [11] K. Chakradeo, M. Delves and S. Titarenko, “Malaria parasite detection using deep learning methods,” *International Journal of Computer and Information Engineering*, vol. 15, no. 2, pp. 175–182, 2021.

- [12] K. M. F. Fuhad, J. F. Tuba, M. R. A. Sarker, S. Momen, N. Mohammed *et al.*, “Deep learning based automatic malaria parasite detection from blood smear and its smartphone based application,” *Diagnostics*, vol. 10, no. 5, pp. 329, 2020.
- [13] D. Shah, K. Kawale, M. Shah, S. Randive and R. Mapari, “Malaria parasite detection using deep learning: (Beneficial to humankind),” in *2020 4th Int. Conf. on Intelligent Computing and Control Systems (ICICCS)*, Madurai, India, pp. 984–988, 2020.
- [14] S. Li, Z. Du, X. Meng and Y. Zhang, “Multi-stage malaria parasite recognition by deep learning,” *GigaScience*, vol. 10, no. 6, pp. giab040, 2021.
- [15] A. Rahman, H. Zunair, T. R. Reme, M. S. Rahman and M. R. C. Mahdy, “A comparative analysis of deep learning architectures on high variation malaria parasite classification dataset,” *Tissue and Cell*, vol. 69, pp. 101473, 2021.
- [16] W. Swastika, G. M. Kristianti and R. B. Widodo, “Effective preprocessed thin blood smear images to improve malaria parasite detection using deep learning,” *Journal of Physics: Conference Series*, vol. 1869, no. 1, pp. 012092, 2021.
- [17] Z. Xu, F. R. Sheykhahmad, N. Ghadimi and N. Razmjoooy, “Computer-aided diagnosis of skin cancer based on soft computing techniques,” *Open Medicine*, vol. 15, no. 1, pp. 860–871, 2020.
- [18] S. Gao, M. Cheng, K. Zhao, X. Zhang, M. Yang *et al.*, “Res2net: A new multi-scale backbone architecture,” *IEEE Transactions on Pattern Analysis and Machine Intelligence*, vol. 43, no. 2, pp. 652–662, 2021.
- [19] S. K. Saha, S. P. Ghoshal, R. Kar and D. Mandal, “Cat swarm optimization algorithm for optimal linear phase fir filter design,” *ISA Transactions*, vol. 52, no. 6, pp. 781–794, 2013.
- [20] A. B. Hassanat, M. A. Abbadi, G. A. Altarawneh and A. A. Alhasanat, “Solving the problem of the K parameter in the KNN classifier using an ensemble learning approach,” *International Journal of Computer Science and Information Security*, vol. 12, no. 8, pp. 33–39, 2014.
- [21] A. Maqsood, M. S. Farid, M. H. Khan and M. Grzegorzec, “Deep malaria parasite detection in thin blood smear microscopic images,” *Applied Sciences*, vol. 11, no. 5, pp. 2284, 2021.